

Absolute Rate Coefficients and Branching Percentages for the Reactions of $\text{PO}_x\text{Cl}_y^- + \text{N} (^4\text{S}_{3/2})$ and $\text{PO}_x\text{Cl}_y^- + \text{O} (^3\text{P})$ at 298 K in a Selected-Ion Flow Tube Instrument

John C. Poutsma,[†] Anthony J. Midey,[‡] Timothy H. Thompson, and Albert A. Viggiano*

Space Vehicles Directorate, Air Force Research Laboratory, Hanscom Air Force Base, Massachusetts 01731

Received: June 15, 2006; In Final Form: July 24, 2006

The absolute rate coefficients and product ion branching percentages at 298 K for the reactions of several PO_xCl_y^- species with atomic nitrogen ($\text{N} (^4\text{S}_{3/2})$) and atomic oxygen ($\text{O} (^3\text{P})$) have been determined in a selected-ion flow tube (SIFT) instrument. PO_xCl_y^- ions are generated by electron impact on POCl_3 in a high-pressure source. O atoms are generated by quantitative titration of N atoms with NO, where N atoms are produced by microwave discharge on N_2 . The experimental procedure allows for the determination of rate coefficients for the reaction of the reactant ion with $\text{N} (^4\text{S}_{3/2})$ and $\text{O} (^3\text{P})$ as well as with N_2 and NO. None of the ions react with N_2 or NO, giving an upper limit to the rate coefficient of $<5 \times 10^{-12} \text{ cm}^3 \text{ molecules}^{-1} \text{ s}^{-1}$. POCl_3^- and POCl_2^- do not react with N atoms, giving an upper limit to the rate coefficient of $<1 \times 10^{-11} \text{ cm}^3 \text{ molecules}^{-1} \text{ s}^{-1}$. The major product ion for POCl_3^- and POCl_2^- reacting with O involves loss of Cl from the reactant ion, accounting for $>85\%$ of the products. PO_2^- is a minor product ($\leq 4\%$) from $\text{POCl}_2^- + \text{O}$. Only PO_2Cl^- reacts with both N and O, directly giving PO_2^- and PO_3^- as major products. In addition, calculations of the structures and energies for PO_2N , PO_2N^- , and NCl have been performed at the G3 level of theory to obtain estimates for the energetics of the PO_2Cl^- reactions. PO_2^- , PO_3^- , and PO_2Cl_2^- are all unreactive with both N and O. Comparisons of the reactivity of PO_xCl_y^- ions with O atoms are made to previous reactivity studies of these ions. In particular, routes that yield the very stable PO_2^- and PO_3^- ions are discussed.

Introduction

Phosphorus-containing compounds are of interest because of their use as fertilizers, pesticides, chemical warfare agents, and flame retardants.^{1–6} These compounds have also been used as fuel additives for combustion sources such as hydrogen-fueled scramjets.⁷ Addition of phosphorus oxychloride, POCl_3 , to fuel-rich hydrocarbon flames produced mainly PO_3^- and PO_2^- as terminal ions.^{8,9} In addition, electron attachment to POCl_3 was shown to produce POCl_2^- and POCl_3^- .^{10–12} To understand the transition from the primary electron attachment products of POCl_3 to the stable fully oxygenated anion species, we have studied the chemistry of the phosphorus oxychloride ions reacting with various oxidizing agents in a selected-ion flow tube (SIFT) instrument.^{13,14}

Previous studies in our laboratory concentrated on determining the absolute rate coefficients for several PO_xCl_y^- ions reacting with O_2 and O_3 ¹³ and with H and H_2 .¹⁴ In those studies, it was shown that the primary products of electron attachment to POCl_3 , POCl_3^- , and POCl_2^- did not yield either PO_3^- or PO_2^- as major primary products.¹³ However, the product ion POCl^- obtained from Cl abstraction in the reaction of $\text{H} + \text{POCl}_2^-$ was shown to react with O_2 to yield PO_3^- and with O_3 to yield PO_2^- .¹⁴ Furthermore, PO_2Cl^- , obtained in the ion source from POCl_3 , was shown to react with both O_2 and O_3 to give PO_3^- .¹³

We have extended these studies to investigate the reactions of the PO_xCl_y^- ions with atomic oxygen and atomic nitrogen

in the SIFT at 298 K. These experiments made use of a titration method recently employed in the SIFT to determine absolute rate coefficients for the reaction of O_2^- with O and N.¹⁵ This standard technique involves the generation of oxygen atoms by the quantitative reaction of nitrogen atoms with NO gas in a Pyrex sidearm.¹⁶ Absolute rate coefficients and product ion branching percentages for the reactions of the primary ion of interest with N, O, N_2 , and NO can be determined using this setup. In this manuscript, we report results for the reactions of these species with the following ions: POCl_3^- , POCl_2^- , PO_2Cl^- , PO_2Cl_2^- , PO_2^- , and PO_3^- .

Experimental Section

All experiments were performed at 298 K in a selected-ion flow tube (SIFT) instrument that has been described in detail elsewhere.^{17,18} Briefly, PO_xCl_y^- ions are generated by electron attachment to POCl_3 in a moderate-pressure electron impact ionization source. This method generates the primary ions POCl_3^- and POCl_2^- , as well as the secondary ions PO_2Cl^- and PO_2Cl_2^- .^{10–12,19} To create PO_2^- and PO_3^- in the source, dimethyl phosphite was used. The ions are then focused into a quadrupole mass filter, mass selected, and injected into the flow reactor via a Venturi-type injector. Ions are thermalized by ca. 10^5 collisions with helium buffer gas, $P_{\text{He}} = 0.5$ Torr. Neutral reagents are injected into the center of the flow tube 49 cm before the end of the flow tube and are allowed to react with the mass-selected ion of interest. The product ions and remaining reactant ions are sampled by a small attractive voltage (1–5 V) through a 1-mm orifice in a blunt nose cone into a second quadrupole mass filter for mass analysis. Ions are then detected with an electron multiplier operating in pulse-counting mode.

* Author to whom correspondence should be addressed. E-mail: albert.viggiano@hanscom.af.mil.

[†] Permanent address: Department of Chemistry, The College of William and Mary, Williamsburg, VA 23187.

[‡] Under Contract to the Institute for Scientific Research, Boston College, Chestnut Hill, MA 02467.

TABLE 1: Supplementary Thermochemical Values^a

species	G3 energy 0 K ^b	G3 enthalpy 298 K ^b	$\Delta H_f^{\circ}{}_{298\text{K}}$ (G3) ^c
POCl ₃ ⁻	-1796.73562	-1796.72744	-696
POCl ₂ ⁻	-1336.68570	-1336.67950	-666
PO ₂ Cl ⁻	-951.78979	-951.78440	-705
PO ₂ Cl ₂ ⁻	-1411.93316	-1411.92673	-987
PO ₂ ⁻	-491.72030	-491.71624	-617
PO ₃ ⁻	-566.96044	-566.95590	-922
PO ₂ N ⁻	-546.38843 ^d	-546.38374 ^d	-421
PO ₂ Cl	-951.71097	-951.70595	-499
PO ₂ N	-546.23940 ^d	-546.23448 ^d	-29
PO ₂	-491.59301	-491.58890	-283
CIN	-514.65641 ^d	-514.65301 ^d	325
CIO	-535.12026	-535.11685	108
Cl ₂	-920.07127	-920.06777	-1
Cl ₂ ⁻	-920.16188	-920.15805	-238
Cl ⁻	-460.12360	-460.12124	-233

species	G3 enthalpy (298 K)	$\Delta H_f^{\circ}{}_{298\text{K}}$ (exp) ^{c,e}
P	-341.11643	316
O	-75.03099	249
N	-54.56434	473
Cl	-459.99096	121

^a G3 values in hartrees. ^b Taken from refs 13 and 14. ^c Heats of formation in kJ mol⁻¹. ^d This work. ^e Data taken from ref 23.

Nitrogen atoms are generated via microwave discharge on a flow of N₂ gas in a Pyrex sidearm. The extent of nitrogen dissociation is small (~1%) and can be varied by changing either the N₂ flow rate or the microwave discharge power. Contributions from vibrationally excited N₂ from this setup are negligible because of collisions in the sidearm.^{16,20} Oxygen atoms are generated using a titration method that has been described in detail elsewhere.^{15,16} Briefly, NO gas is introduced at a known flow rate into the Pyrex sidearm downstream of the discharge where it reacts with nitrogen atoms to give ground-state oxygen atoms.¹⁶ The sidearm was treated with a boric acid slurry to minimize O atom losses to the walls of the tube. As NO reacts with N quantitatively to give O atoms, a titration plot of ln-[reactant ion intensity] versus [NO] can be used to determine rate coefficients.

As both NO and N₂ will be present in the flow tube during the titration, the reactions of these two stable species with each reactant ion must be studied first. These are done in the standard manner by measuring the decay, if any, of the reactant ion versus gas concentration. As will be shown, none of the ions reacted with NO or N₂, eliminating any interference from these two compounds. Subsequently, the shape of the titration curve will vary depending on the relative reaction rates of the reactant ion with N and O but should have a discernible end point. The absolute rate coefficient for the reaction of the primary reactant ion with N atoms was obtained from a two-point difference in reactant ion intensity (discharge on and off, both without NO added). The total N and O atom concentrations were determined from the end point of the titration. Thus, the slope of the curve before the end point gives the difference between the O atom and the N atom rate coefficients. The slope after the end point is due to the NO reaction. The uncertainties shown in the following sections and in Table 1 are one sigma on multiple runs. Absolute uncertainties in the rate coefficients are about ±40%; relative rate coefficients are typically ±20% for these experiments.¹⁵

Product ion branching percentages for the reactions of PO_xCl_y⁻ + N were obtained by monitoring the intensity of both the reactant and the products as a function of either the microwave discharge power or the N₂ flow. Product branching ratios were obtained at varying nitrogen atom concentrations

and then were extrapolated to zero concentration to minimize contributions from any secondary reactions of the product ions. For those ions that did not react with N atoms, branching ratios for PO_xCl_y⁻ + O were obtained in a similar manner, except that the O atom concentration was scanned by varying the NO flow over the course of the titration, followed by the extrapolation. Branching percentages for POCl₂⁻ are reported as upper and lower limits, reflecting the fact that the primary PO₂Cl⁻ product also reacts with both N and O to give similar product ions as the POCl₂⁻ reaction. This secondary chemistry contribution to the observed product ion signals could be corrected for in a limited way by subtracting the background contributions and renormalizing the product distribution using the corrected product ion intensities. The branching percentages for the PO₂Cl⁻ and POCl₂⁻ reactions were further refined by additional product branching percentage measurements using a 10% NO in He mixture to perform the titration. This approach permitted lower NO concentrations in the flow tube, further minimizing contributions from the secondary chemistry. This method also minimized possible contributions from trace impurities that might not have been sufficiently removed from higher flows of neat NO if the sieve trap was saturated.

To assist in understanding the observed chemistry, energies at 0 K and enthalpies at 298 K were obtained for optimized structures of PO₂N, PO₂N⁻, and NCl using the G3 methodology.²¹ All calculations were performed using the Gaussian 03W suite of programs.²² Heats of formation for these species were obtained from the total atomization energy approach using 298 K heats of formation for the elements.²³

Materials

Dimethyl phosphite (Ventron, 99%) and POCl₃ (Aldrich, 99%) were used as supplied, except for being subjected to several freeze-pump-thaw cycles with liquid N₂. Reagent gases (N₂, O₂, and NO) were also used as supplied, except that the neat NO reagent gas was passed through molecular sieves in a liquid nitrogen/methanol slush bath maintained between -80 to -100 °C. Gas purities were as follows: N₂ (AGA, 99.999%), O₂ (Mass. Oxygen, 99.999%), NO (Matheson, 99%), and He (AGA, 99.999%). The use of 99.999% N₂ was essential for these studies as outlined previously.

Results

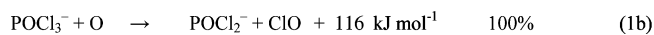
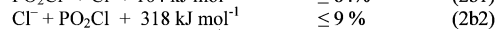
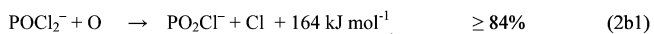
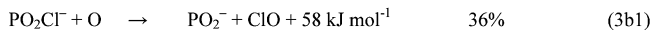
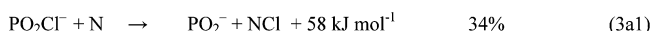
None of the ions studied here reacted with either N₂ or NO. Consequently, an upper limit of <5 × 10⁻¹² cm³ molecule⁻¹ s⁻¹ can be placed on the rate coefficients for the reactions with N₂ and NO. The reactivity of the various ions with N and O will be discussed individually in detail below. The heats of reaction given below were calculated using the G3 enthalpies at 298 K reprinted in Table 1 from refs 13 and 14, except for the values of NCl, PO₂N, and PO₂N⁻, which will be discussed below. The experimental kinetics results are summarized in Table 2.

(a) **POCl₃⁻**. The reactivity of the parent ion POCl₃⁻ with N and O is shown in Scheme 1, along with the calculated reaction energetics for the observed channels. Absolute rate coefficients for all of the channels are given in Table 2. No reaction products or decay of the POCl₃⁻ ion occurred with the presence of N atoms. Consequently, an upper limit of <1 × 10⁻¹¹ cm³ molecule⁻¹ s⁻¹ can be placed on the rate coefficient for the reaction of POCl₃⁻ + N. This limit is higher than with stable gases such as N₂ because of the lower total concentration of atoms produced (i.e., 1% of [N₂]). In contrast, POCl₃⁻ reacted

TABLE 2: Measured Rate Coefficients and Branching Ratios for Reactions of PO_xCl_y^- Ions with N, O, NO, and N_2 at 298 K^a

reaction	products	k ($\times 10^{-10}$) cm^3 $\text{molecules}^{-1} \text{s}^{-1}$	k_{col} ($\times 10^{-10}$) cm^3 $\text{molecules}^{-1} \text{s}^{-1}$
$\text{POCl}_3^- + \text{N}$		no reaction	
$\text{POCl}_3^- + \text{O}$	$\text{POCl}_2^- + \text{ClO}$	100%	3.9 ± 0.8
$\text{POCl}_3^- + \text{NO}$		no reaction	
$\text{POCl}_3^- + \text{N}_2$		no reaction	
$\text{POCl}_2^- + \text{N}$		no reaction	
$\text{POCl}_2^- + \text{O}$	$\text{PO}_2\text{Cl}^- + \text{Cl}$	$\geq 84\%$	3.7 ± 0.6
	$\text{Cl}^- + \text{PO}_2\text{Cl}$	$\leq 9\%$	
	$\text{PO}_2^- + \text{Cl}_2$	$\leq 4\%$	
	$\text{Cl}_2^- + \text{PO}_2$	$\leq 3\%$	
$\text{POCl}_2^- + \text{NO}$		no reaction	
$\text{POCl}_2^- + \text{N}_2$		no reaction	
$\text{PO}_2\text{Cl}^- + \text{N}$	$\text{PO}_2^- + \text{NCl}$	34%	0.80 ± 0.28
	$\text{PO}_2\text{N}^- + \text{Cl}$	66%	
$\text{PO}_2\text{Cl}^- + \text{O}$	$\text{PO}_2^- + \text{ClO}$	36%	2.6 ± 0.2
	$\text{PO}_3^- + \text{Cl}$	64%	
$\text{PO}_2\text{Cl}^- + \text{NO}$		no reaction	
$\text{PO}_2\text{Cl}^- + \text{N}_2$		no reaction	

^a The uncertainty shown is one sigma on multiple runs; the total uncertainty is $\pm 40\%$.

SCHEME 1**SCHEME 2****SCHEME 3**

with oxygen atoms to yield POCl_2^- as the exclusive primary product, as shown in reaction Scheme 1.

As POCl_3^- did not react with N atoms, the rate coefficient for its reaction with O was directly obtained from the slope of the curve before the end point, which yielded a rate coefficient of $3.9 \pm 0.8 \times 10^{-10} \text{ cm}^3 \text{ molecules}^{-1} \text{ s}^{-1}$. The uncertainty shown is one sigma on multiple runs; the total uncertainty is $\pm 40\%$. The same applies to all quoted error limits in the following sections.

(b) POCl_2^- . Similarly to POCl_3^- , POCl_2^- did not react with atomic nitrogen to give discernible products. Again, there was no reduction of primary ion signal upon addition of nitrogen atoms, indicating a rate coefficient of $< 1 \times 10^{-11} \text{ cm}^3 \text{ molecule}^{-1} \text{ s}^{-1}$. Scheme 2 summarizes the observed chemistry for POCl_2^- , and the absolute rate coefficients for the observed reactions are shown in Table 2.

POCl_2^- was found to react with oxygen atoms to give several primary product ions. Unfortunately, the most abundant of these, PO_2Cl^- , also reacted efficiently with N and O to give a variety of overlapping secondary products (vide infra). The corrected branching ratios for reactions 2b1–4 are given as upper and lower limits as previously discussed. As with POCl_3^- , there was no reaction with nitrogen atoms; therefore, the oxygen atom

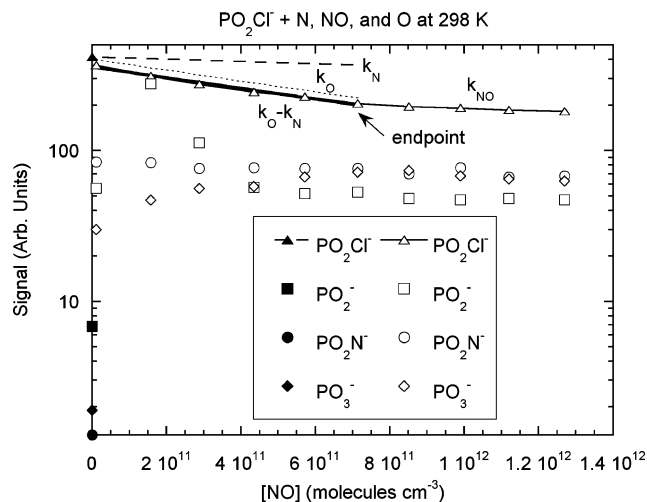


Figure 1. Titration plot of reactant and product ion signals versus $[\text{NO}]$. Closed symbols indicate data with the microwave discharge off; open symbols (\diamond) indicate data with microwave discharge on. End point of plot is shown with an arrow. Solid lines are fits to experimental data. Dashed line and dotted line are used to obtain rate coefficients for reaction with nitrogen and oxygen atoms, respectively, as discussed in text.

rate coefficient was again determined from the slope of the titration curve before the end point. The overall rate coefficient for reaction of POCl_2^- with oxygen atoms was determined to be $3.7 \pm 0.8 \times 10^{-10} \text{ cm}^3 \text{ molecule}^{-1} \text{ s}^{-1}$. Interestingly, channels 2b1 and 2b2 differ only in the location of the charge on the product; yet, the least exothermic channel is by far dominant. No obvious reason for this observation was apparent, but it implied that once the product ion formed, the electron was not readily exchanged.

(c) PO_2Cl^- . Electron impact on a sample of POCl_3 in the moderate-pressure source produced abundant signal for the PO_2Cl^- anion via source chemistry at high energy. PO_2Cl^- was allowed to react with N and O in a similar manner as POCl_3^- and POCl_2^- , and the energetics for the observed products are given in Scheme 3. In contrast to POCl_3^- and POCl_2^- , PO_2Cl^- did react slowly with atomic nitrogen to give two primary products, PO_2^- and PO_2N^- .

PO_2Cl^- also reacted with oxygen atom to give PO_2^- and PO_3^- as primary products. A titration curve for these reactions is shown in Figure 1. A two-point rate determination for the nitrogen reaction led to a rate coefficient of $8.0 \pm 2.8 \times 10^{-11} \text{ cm}^3 \text{ molecule}^{-1} \text{ s}^{-1}$. Combining this rate coefficient with the difference in the oxygen and nitrogen rate coefficients obtained from the slope before the end point gives a rate coefficient for the oxygen reaction of $2.6 \pm 0.2 \times 10^{-10} \text{ cm}^3 \text{ molecule}^{-1} \text{ s}^{-1}$. Separate experiments were performed to monitor the reaction of PO_2Cl^- with NO, and no products were observed. Thus, the small decline after the end point in Figure 1 reflects a small unknown experimental artifact, possibly an additional fast reaction with trace impurities created in the discharge with NO addition. A small signal drift because of ion-sampling effects in the presence of O atoms could also account for this decay, where a small drift could exacerbate the difficulty in observing rate coefficients near the SIFT detection limit.

(d) Calculations for PO_2N^- , PO_2N , and NCl. No experimental values could be found in the literature for the thermochemical properties of PO_2N^- and PO_2N . Consequently, calculations of the 0 K energy, 298 K enthalpy, and standard heat of formation at 298 K were performed for optimized geometries at the G3 level of theory²¹ using Gaussian 03W. The calculated

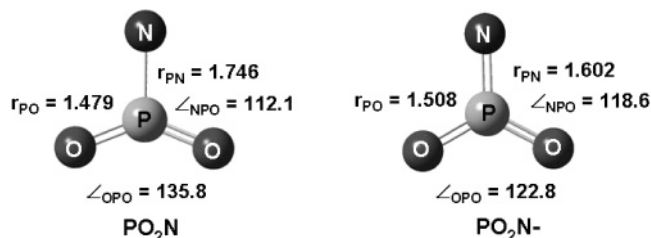


Figure 2. Optimized structural parameters for NPO_2 (${}^3\text{A}_2$, C_{2v}) and NPO_2^- (${}^2\text{B}_2$, C_{2v}) calculated at the HF/6-31G(d) level as part of G3 calculations. See text for details.

energetics are shown in Table 1. Optimizations were performed for a wide range of possible isomers. The minimum energy structures for PO_2N and PO_2N^- were both planar C_{2v} structures with the phosphorus as the central atom, having the structural parameters shown in Figure 2. The P–N bond was a single bond in PO_2N but contracted in the PO_2N^- ion to a P–N double bond. Both P–O bonds were double bonds in the neutral and the anion. The wave function stability of both optimized minimum energy structures was verified at the Hartree–Fock HF/6-31G(d) level of the G3 structure optimization step. The mean absolute deviation in heats of formation calculated using the G3 theory is ± 4 kJ mol $^{-1}$.

Two other stable planar PO_2N structures were also found that were both around 16 kJ mol $^{-1}$ higher in energy. These species had a planar OPNO arrangement, one with the two terminal O atoms cis and the other with the O atoms trans to each other. A third stable planar PNO $_2$ arrangement with the N as the central atom was about 241 kJ mol $^{-1}$ higher in energy than the minimum energy structure.

Two other stable PO_2N^- structures were also found. One structure had a cyclic PNO arrangement with the other out-of-plane O atom double bonded to the phosphorus atom, lying 174 kJ mol $^{-1}$ higher in energy. The other structure had the planar PNO $_2$ arrangement with the N as the central atom lying over 385 kJ mol $^{-1}$ higher in energy.

The G3 heat of formation for NCl at 298 K calculated here was 325 kJ mol $^{-1}$. The NCl bond dissociation energy of the ground electronic state was determined by Xantheas et al. by extrapolations to the complete basis set (CBS) limit from coupled cluster calculations at the RCCSD(T) level using both cc-pVxZ and aug-cc-pVxZ basis sets for $x = 2-6$ then adding core–valence correlation effects.²⁴ These calculations represented the highest level of theory that had been applied to this molecule and gave a bond dissociation energy of 270.3 ± 5.4 kJ mol $^{-1}$, indicating that the previous experimental values of 326–335 kJ mol $^{-1}$ were suspect. The experimental determinations were estimated from chemiluminescent and mass spectrometric detection of NCl in discharge-flow system kinetics experiments.^{25–27} Using the bond energy of Xantheas et al. and the heats of formation at 298 K for N and Cl atoms²³ gave a heat of formation for NCl at 298 K of 323.7 kJ mol $^{-1}$, in excellent agreement with the value derived from the current G3 calculations.

(e) PO_2Cl_2^- , PO_2^- , and PO_3^- . PO_2Cl_2^- , PO_2^- , and PO_3^- were also subjected to reactivity studies with N_2 , NO, N, and O. None of these ions reacted to give discernible products or reactant ion decay. This observation is consistent with previous experiments on the reactivity of PO_2^- and PO_3^- , which showed that these two ions were unreactive with N_2 and NO.²⁸

Discussion

Comparisons of Reactivity. A comparison can be made between the reactivity of the two primary ions POCl_3^- and

POCl_2^- that are generated by electron attachment to POCl_3 .^{10,11} POCl_3^- reacted with atomic oxygen only via chloride atom extraction to give ClO, whereas POCl_2^- did not undergo this abstraction reaction, as it is more than 125 kJ mol $^{-1}$ endothermic. Instead, POCl_2^- reacted with atomic oxygen by addition of an O with concomitant loss of a Cl atom in a similar reaction to that seen for PO_2Cl^- with both O and N (vide infra). POCl_2^- also produces a small amount of Cl^- product, as the electron affinities of POCl_2^- and Cl are comparable, that is, 367 and 347 kJ mol $^{-1}$, respectively. These two products accounted for >93% of the observed products, although a small amount of PO_2^- was also generated directly from POCl_2^- .

A second observation was that the PO_xCl_y^- ions were essentially unreactive with nitrogen atoms. Only the PO_2Cl^- ion reacted with nitrogen atoms to a measurable extent. This reaction was somewhat inefficient ($k/k_{\text{col}} = 0.11$, where k_{col} is the Langevin collision rate coefficient) but did lead to a small amount of PO_2^- as a minor end product. The major product ion PO_2N^- resulted from addition of N with loss of Cl. A similar reaction occurred in the reaction of PO_2Cl^- with oxygen atoms to give PO_3^- as the major product.

Comparing the rate coefficients for the reactions of PO_xCl_y^- with O_3 , O, and H shows that the O atom reactions are much more efficient than the H atom reactions, but their efficiencies are comparable to the efficiencies for the O_3 reaction in most cases. The rate coefficients for the reactions of O_3 and O are >50% of the collision rate constant for PO_2Cl^- and POCl_3^- . The reaction of POCl_2^- with O was much more efficient ($k/k_{\text{col}} = 0.66$) than the reactions with O_3 (0.13) and H (0.08).

Production of PO_2^- and PO_3^- Products. One of the primary goals of this work was to further the understanding of the mechanisms for formation of PO_2^- and PO_3^- ions from the addition of POCl_3 to hydrocarbon flames.^{8,9} The primary ions that arise upon electron attachment to POCl_3 in high-pressure flames would be POCl_3^- and POCl_2^- .^{10,11} In previous studies from our laboratory of the reactions of PO_xCl_y^- with O_2 , O_3 , and H, it was shown that production of the PO_2^- and PO_3^- end products came primarily from reactions of the minor ionic species PO_2Cl^- and POCl^- rather than directly from the primary ions POCl_3^- or POCl_2^- .^{13,14} POCl^- was produced from efficient chloride atom abstraction in the reaction of hydrogen atom with POCl_2^- . This product ion could then react slowly with O_2 ($k = 9 \times 10^{-11}$) and quickly with O_3 ($k = 5 \times 10^{-10}$) to form PO_2^- and PO_3^- . It was therefore postulated that the reaction of $\text{POCl}_2^- + \text{H}$ was a key first step in the production of these important end products.¹⁴

Figure 3 shows a graphical summary of the reactions of PO_xCl_y^- with H, N, O, O_2 , O_3 , and POCl_3 compiled from the current results and the previous kinetics studies.^{10,12–14,19} The reaction efficiencies for each pathway are shown in parentheses, defined as the product of the branching fraction with the ratio of observed rate constant, k , to the collision rate constant, k_{col} . As can be seen from the figure, there are several viable routes to the PO_2^- and PO_3^- terminal ions. Similar trends in the chemistry were observed in this study of the O atom reactions as were found in previous work^{13,14} in that neither primary ion POCl_3^- nor POCl_2^- reacted to directly give PO_2^- or PO_3^- as major product ions. Rather, POCl_3^- reacted with oxygen atoms by chloride atom transfer to give POCl_2^- that, in turn, reacted with O atoms to give the secondary product PO_2Cl^- . It was this ion that reacted with oxygen atoms to directly give PO_2^- and PO_3^- end products. Both reactions 1b and 2b1 are fairly efficient, that is, 71 and >56% of the respective Langevin collision rates; thus, there should be an ample concentration of

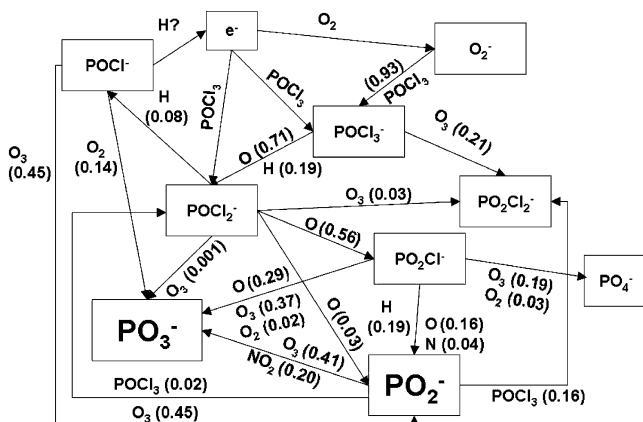


Figure 3. Chemical cycle for producing PO_2^- and PO_3^- beginning with electrons, O_2 , and POCl_3 . The numbers in parentheses are reaction efficiencies defined as the ratio of rate constant k measured to the collision rate constant, k_{col} . The data for reactions of PO_xCl_y^- ions with O_2 , O_3 , and H are from refs 13 and 14.

the secondary ion PO_2Cl^- available for further reaction with O atoms in the flame. This step should therefore compete with $\text{POCl}^- + \text{H}$ as a possible first step in the generation of PO_2^- and PO_3^- end products. Subsequently, these combined studies showed some prominent pathways from the primary electron attachment anions to the stable terminal ions. However, other routes involving PO_xCl_y neutral molecules generated in the flames probably supplement the observed chemistry.

Conclusions

The rate coefficients and production ion branching percentages for PO_xCl_y^- ions reacting with N_2 , NO , N , and O were measured at 298 K in a SIFT through titration of N atoms produced in a microwave discharge with NO to quantitatively generate O atoms. None of the ions reacted with N_2 or NO , having an upper limit to the rate coefficient of $<5 \times 10^{-12}$ cm^3 molecules $^{-1}$ s^{-1} . POCl_2^- and POCl_3^- did not react with N atoms; an upper limit to the rate coefficients with N of $<1 \times 10^{-11}$ cm^3 molecules $^{-1}$ s^{-1} can be given. These ions did react with O atoms, giving primarily loss of Cl as part of the reaction process. PO_2^- was only observed as a minor primary product ion in the reaction of POCl_2^- with O . PO_2Cl^- reacted with both N and O , providing a direct route to PO_3^- and PO_2^- as seen in previous experiments with O_3 and H .^{13,14} The current results can be combined with the previous kinetics measurements in the SIFT with PO_xCl_y^- to give a detailed picture of the complicated chemical scheme that describes how POCl_3 in the presence of electrons in a combustion environment leads to the major terminal ions PO_2^- and PO_3^- observed.

Acknowledgment. A.A.V. and A. J. M. are supported by the United States Air Force Office of Scientific Research (AFOSR) under Project No. 2303EP4. A. J. M. is supported under contract No. FA8718-04-C-0006 to Boston College. J. C. P. was supported on a Summer Faculty Grant from the American Society of Engineering Education.

References and Notes

- (1) Corbridge, D. E. C. *Phosphorus: An Outline of its Chemistry, Biochemistry, and Technology*, 3rd ed.; Elsevier: Amsterdam, 1980; Vol. 6.
- (2) *The Pesticide Manual*, 13th ed.; British Crop Protection Council: Alton Hampshire, U.K., 2003.
- (3) *Handbook of Plasticizers*, 1st ed.; Chem Tec.: Toronto, Canada, 2004.
- (4) Price, D.; Pyrah, K.; Hull, T. R.; Milnes, G. J.; Ebdon, J. R.; Hunt, B. J.; Joseph, P. *Polym. Degrad. Stab.* **2002**, *77*, 227.
- (5) *Handbook or Hydraulic Fluid Power Technology*; Marcel Dekker: New York, 2000.
- (6) Korobeinichev, O. P.; Ilyin, S. B.; Bolshova, T. A.; Shvartsberg, V. M.; Chernov, A. A. *Combust. Flame* **2000**, *121*, 593.
- (7) Pellett, G. L. *NASA Tech. Rep.* 1996, 1.
- (8) Goodings, J. M.; Hassanali, C. S. *Int. J. Mass Spectrom. Ion Processes* **1990**, *101*, 337.
- (9) Horton, J. H.; Crovisier, P. N.; Goodings, J. M. *Int. J. Mass Spectrom. Ion Processes* **1992**, *114*, 99.
- (10) Miller, T. M.; Seeley, J. V.; Knighton, W. B.; Meads, R. F.; Viggiano, A. A.; Morris, R. A.; Van Doren, J. M.; Gu, J.; Schaefer, H. F., III. *J. Chem. Phys.* **1998**, *109*, 578.
- (11) Williamson, D. H.; Mayhew, C. A.; Knighton, W. B.; Grimsrud, E. P. *J. Chem. Phys.* **2000**, *113*, 11035.
- (12) Van Doren, J. M.; Friedman, J. F.; Miller, T. M.; Viggiano, A. A.; Denifl, S.; Scheier, P.; Mark, T. D.; Troe, J. *J. Chem. Phys.* **2006**, *124*, DOI: 124322.
- (13) Fernandez, A. I.; Midey, A. J.; Miller, T. M.; Viggiano, A. A. *J. Phys. Chem. A* **2004**, *108*, 9120.
- (14) Midey, A. J.; Miller, T. M.; Morris, R. A.; Viggiano, A. A. *J. Phys. Chem. A* **2005**, *109*, 2559.
- (15) Poutsma, J. C.; Midey, A. J.; Viggiano, A. A. *J. Chem. Phys.* **2006**, *124*, 074301.
- (16) Viggiano, A. A.; Howorka, F.; Albritton, D. L.; Fehsenfeld, F. C.; Adams, N. G.; Smith, D. *Astrophys. J.* **1980**, *236*, 492.
- (17) Viggiano, A. A.; Morris, R. A.; Dale, F.; Paulson, J. F.; Giles, K.; Smith, D.; Su, T. *J. Chem. Phys.* **1990**, *93*, 1149.
- (18) Viggiano, A. A.; Morris, R. A. *J. Phys. Chem.* **1996**, *100*, 19227.
- (19) Morris, R. A.; Viggiano, A. A. *Int. J. Mass Spectrom. Ion Processes* **1997**, *164*, 35.
- (20) Schmeltekopf, A. L.; Ferguson, E. E.; Fehsenfeld, F. C. *J. Chem. Phys.* **1968**, *48*, 2966.
- (21) Curtiss, L. A.; Raghavachari, K.; Redfern, P. C.; Rassolov, V.; Pople, J. A. *J. Chem. Phys.* **1998**, *109*, 7764.
- (22) Frisch, M. J.; Trucks, G. W.; Schlegel, H. B.; Scuseria, G. E.; Robb, M. A.; Cheeseman, J. R.; Montgomery, J. A., Jr.; Vreven, T.; Kudin, K. N.; Burant, J. C.; Millam, J. M.; Iyengar, S. S.; Tomasi, J.; Barone, V.; Mennucci, B.; Cossi, M.; Scalmani, G.; Rega, N.; Petersson, G. A.; Nakatsuji, H.; Hada, M.; Ehara, M.; Toyota, K.; Fukuda, R.; Hasegawa, J.; Ishida, M.; Nakajima, T.; Honda, Y.; Kitao, O.; Nakai, H.; Klene, M.; Li, X.; Knox, J. E.; Hratchian, H. P.; Cross, J. B.; Adamo, C.; Jaramillo, J.; Gomperts, R.; Stratmann, R. E.; Yazyev, O.; Austin, A. J.; Cammi, R.; Pomelli, C.; Ochterski, J. W.; Ayala, P. Y.; Morokuma, K.; Voth, G. A.; Salvador, P.; Dannenberg, J. J.; Zakrzewski, V. G.; Dapprich, S.; Daniels, A. D.; Strain, M. C.; Farkas, O.; Malick, D. K.; Rabuck, A. D.; Raghavachari, K.; Foresman, J. B.; Ortiz, J. V.; Cui, Q.; Baboul, A. G.; Clifford, S.; Cioslowski, J.; Stefanov, B. B.; Liu, G.; Liashenko, A.; Piskorz, P.; Komaromi, I.; Martin, R. L.; Fox, D. J.; Keith, T.; Al-Laham, M. A.; Peng, C. Y.; Nanayakkara, N.; Challacombe, M.; Gill, P. M. W.; Johnson, B.; Chen, W.; Wong, M. W.; Gonzalez, C.; Pople, J. A. *Gaussian 03W*, revision B.02 ed.; Gaussian, Inc: Pittsburgh, PA, 2003.
- (23) Lias, S. G.; Bartmess, J. E.; Liebman, J. F.; Homes, J. F.; Levin, J. L.; Mallard, W. D. *J. Phys. Chem. Ref. Data* **1988**, *17*, Suppl. 1.
- (24) Xantheas, S. S.; Dunning, J. T. H.; Mavridis, A. *J. Chem. Phys.* **1997**, *106*, 3280.
- (25) Clark, T. C.; Clyne, M. A. A. *Trans. Faraday Soc.* **1970**, *66*, 877.
- (26) Clyne, M. A. A.; MacRobert, A. J. *J. Chem. Soc., Faraday Trans. 2* **1983**, *79*, 283.
- (27) Clyne, M. A. A.; MacRobert, A. J.; Stief, L. J. *J. Chem. Soc., Faraday Trans. 2* **1985**, *81*, 159.
- (28) Morris, R. A.; Viggiano, A. A. *J. Chem. Phys.* **1998**, *109*, 4126.